J|A|C|S ARTICLES

Published on Web 11/09/2010

Atomistic Evidence of How Force Dynamically Regulates Thiol/Disulfide Exchange

Wenjin Li[†,‡] and Frauke Gräter*[,†,‡]

CAS-MPG Partner Institute and Key Laboratory for Computational Biology, Shanghai Institutes for Biological Sciences, Chinese Academy of Sciences, 320 Yue Yang Road, Shanghai 200031, China, and Heidelberg Institute for Theoretical Studies, Schloss-Wolfsbrunnenweg 35, 69118 Heidelberg, Germany

Received June 1, 2010; E-mail: frauke.graeter@h-its.org

Abstract: The intricate coupling of mechanical force and chemical reactivity has been increasingly revealed in recent years by force spectroscopy experiments on the thiol/disulfide exchange reaction. We here aimed at elucidating the underlying dynamic effects of force on the reaction center for the case of disulfide bond reduction by dithiothreitol at forces of 200−2000 pN, by combining transition path sampling and quantum/classical mechanical simulations. Reaction rates and their dependence on force as quantified by Δx_r, the distance between reactant and transition state, are in good agreement with experiments but indicate a shift of the transition state structure at high forces. Indeed, while an associate S_N2 mechanism prevails, force causes a move of the transition state to a longer length of the cleaving bond and a shorter length of the forming disulfide bond. Our results highlight the distribution of force into various degrees of freedom, which implies that care must be taken when correlating Δx_r with a single order parameter of the reaction.

1. Introduction

Mechanical force has been discovered to activate and regulate chemical reactions similar to the more classical catalysts heat, electrons, and protons. In recent years, experimental approaches have been devised to measure the impact of mechanical force on bond cleavage and bond rotation reactions.[1−4] One of the milestones in this field was the study of thiol/disulfide exchange using force clamp spectroscopy,[3] a technique based on atomic force microscopy that allows us to hold a single molecule at a constant force and to monitor its changes in length during a reaction. The reaction rate of disulfide bond reduction in an engineered immunoglobulin domain of titin (I27) by various chemical reducing agents like dithiothreitol (DTT) was found to exponentially increase with the applied mechanical force.[3,5] However, for a large range of forces (>500 pN), or for enzymes or metal ions as reducing agents, mechanical force was observed to regulate the reaction kinetics in a more complex way, featuring variations in the force-induced acceleration, or even fully force-independent kinetics.[6] In other cases, an intricate combination of a decrease and increase of reactivity with force was observed.[7,8]

The analysis and interpretation of these force-clamp experiments were based on the Bell model, a simple relation that predicts a rate to exponentially increase with the applied work, $F\Delta x_r$, where F is the force and Δx_r is the distance between the transition state (TS) and reactant state (RS) along the pulling reaction.[9] It has been originally formulated for and applied to noncovalent bond rupture, such as receptor−ligand detachment or protein unfolding.[10] This model assumes that the reaction coordinate is parallel to the pulling force, and thus is well described by the end-to-end distance of the system, and that Δx_r is force-independent; i.e., the positions of RS and TS do not change with force. Extensions of this model based on Kramer's theory of diffusive barrier crossing have been devised to account for shifts in TS toward RS due to the force tilting the free energy landscape.[11] Experiments showing deviations from a single exponential force-dependency for proteins unfolding[12] and DNA unzipping[13] could be well fitted with this Dudko model. The fundamental question arises if a force-regulated chemical reaction such as the cleavage of a covalent bond fulfills the basic premises of these models. More specifically, is the reaction coordinate well described by the end-to-end distance

[†] CAS-MPG Partner Institute and Key Laboratory for Computational Biology.

[‡] Heidelberg Institute for Theoretical Studies.

(1) Grandbois, M.; Beyer, M.; Rief, M.; Clausen-Schaumann, H.; Gaub, H. E. *Science* **1999**, *283*, 1727–1730.
(2) Hickenboth, C. R.; Moore, J. S.; White, S. R.; Sottos, N. R.; Baudry, J.; Wilson, S. R. *Nature* **2007**, *446*, 423–427.
(3) Wiita, A. P.; Ainavarapu, S. R.; Huang, H. H.; Fernandez, J. M. *Proc. Natl. Acad. Sci. U.S.A.* **2006**, *103*, 7222–7227.
(4) Beyer, M. K.; Clausen-Schaumann, H. *Chem. Rev.* **2005**, *105*, 2921–2948.
(5) Koti Ainavarapu, S. R.; Wiita, A. P.; Dougan, L.; Uggerud, E.; Fernandez, J. M. *J. Am. Chem. Soc.* **2008**, *130*, 6479–6487.
(6) Garcia-Manyes, S.; Liang, J.; Szoszkiewicz, R.; Kuo, T.; Fernández, J. *Nat. Chem.* **2009**, *1*, 236–242.
(7) Wiita, A. P.; Perez-Jimenez, R.; Walther, K. A.; Graeter, F.; Berne, B. J.; Holmgren, A.; Sanchez-Ruiz, J. M.; Fernandez, J. M. *Nature* **2007**, *450*, 124–127.
(8) Perez-Jimenez, R.; et al. *Nat. Struct. Mol. Biol.* **2009**, *16*, 890–896.
(9) Bell, G. I. *Science* **1978**, *200*, 618–627.
(10) Rief, M.; Gautel, M.; Oesterhelt, F.; Fernandez, J. M.; Gaub, H. E. *Science* **1997**, *276*, 1109–1112.
(11) Dudko, O. K.; Hummer, G.; Szabo, A. *Phys. Rev. Lett.* **2006**, *96*, 108101.
(12) Schlierf, M.; Rief, M. *Biophys. J.* **2006**, *90*, L33–35.
(13) Dudko, O. K.; Hummer, G.; Szabo, A. *Proc. Natl. Acad. Sci. U.S.A.* **2008**, *105*, 15755–15760.

 10.1021/ja104763q

of the system? And does the force regulate the reaction by propagating solely along this single dimension among the many degrees of freedom of the system? Assessing Δx_r at the atomic level, including quantum and dynamic effects, is required.

Recently, quantum mechanical simulations were applied to evaluate the activation energy (ΔE_a) for the ring-opening of a cyclobutene derivative. The authors reported a change in the reaction paths with force and as a consequence a shortening in the distance between RS and TS on the potential energy landscape.[14] Here, we investigated the bimolecular reaction of disulfide bond reduction under forces ranging from 200 pN to 2 nN. The thiol/disulfide exchange reaction is a biologically important process involved in protein folding and function,[15,16] and the characteristics of its transition state have been extensively studied in recent years.[17,18] Most importantly, its behavior under mechanical force was experimentally quantified as mentioned above.[3] As in the pioneering experiments, we studied the reaction of I27 with DTT in water, and to this end combines transition path sampling (TPS)[19] and quantum mechanical and molecular mechanical (QM/MM) simulations,[20] as these techniques recently proved useful to study enzymatic catalysis.[21] On the basis of a total simulation time of 20 ns (about 6×10^5 central processing unit (CPU) hours), force-dependent rate constants were estimated, quantitatively compared to experiments, and found not to follow a single-exponential increase with force. The ensemble of transition paths is in agreement with previous CPMD simulations of the same reaction under high pulling velocities.[22]

In this study, for the first time, we resolve a force-induced shift in the TS ensemble of a reaction visited in dynamic trajectories, i.e. on the free energy landscape, at the atomic level. Δx_r, which usually is referred to as the distance from TS to RS along the pulling coordinate, was interpreted only as the projection of a multidimensional reaction coordinate onto the pulling direction. In other words, our results suggest force to distribute through the highly dimensional reaction system in a more complex way than previously envisioned.

2. Methods

2.1. Molecular Dynamics (MD) Simulations. All simulations were carried out with the software suite GROMACS-3.3.1.[23] The OPLS all atom force field[24] was applied. Simulations were run in the NpT ensemble with periodic boundary conditions. The temperature of the system was kept constant at $T = 300$ K by coupling to the Nose−Hoover thermostat[25,26] with $\tau_t = 0.1$ ps. The pressure was kept constant at $p = 1$ bar using isotropic coupling to a Parrinello−Rahman barostat with $\tau_p = 1.0$ ps and a compressibility of 4.5×10^{-5} bar^{-1} in x, y, and z directions.[27,28] Lennard−Jones interactions were calculated using a cutoff of 10 Å. At a distance smaller than 10 Å, electrostatic interactions were calculated explicitly, whereas long-range electrostatic interactions were calculated by particle-mesh Ewald summation.[29] An integration time step of 2 fs was used, and all bonds were constrained using LINCS,[30] if not noted otherwise.

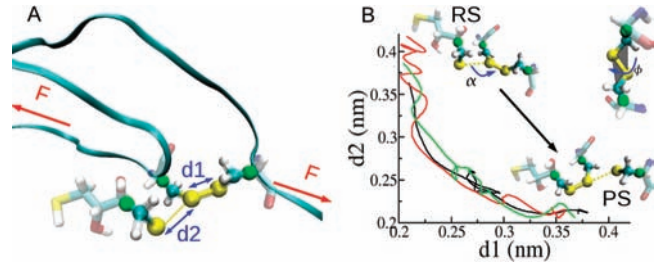

Figure 1. QM/MM setup and pathways of the thiol/disulfide exchange between DTT and $I27_{SS}^{trunc}$. (A) A snapshot of the simulation system. $I27_{SS}^{trunc}$ is shown as a blue ribbon, two cysteines between which the disulfide bond forms, and DTT are shown as licorice. The QM part is highlighted as spheres, the three sulfur atoms are shown as yellow spheres, and three link atoms are shown as green spheres. The solvent and ions are not shown for clarity. (B) Three typical examples of transition paths at 200 pN projected onto $d1$ and $d2$. $d1$ and $d2$ are the lengths of the old and new disulfide bond, respectively, and are indicated by blue arrows in A. The attacking angle α and the dihedral near the old disulfide bond ϕ are also indicated in B.

A disulfide bonded mutant, $I27_{SS}$ with cysteines at positions 32 and 75 (PDB accession number of the wild-type I27 is 1TIT), was generated, equilibrated, and mechanically unfolded as previously described.[7] To reduce the system size for subsequent simulations, the unfolded fragments of the protein distant from the disulfide bond were removed and only residues 27−42 and 63−80 of $I27_{SS}$ were kept. A singly deprotonated DTT molecule was placed next to the truncated $I27_{SS}^{trunc}$ disulfide bond, with the thiolate sulfur pointing toward the CYS32 sulfur (Figure 1A). The protein and DTT were solvated in a $5.0 \times 4.8 \times 8.3$ nm^3 box of TIP4P water, and ions were added. An energy minimization of 1000 steps using the steepest descent algorithm was followed by a 1 ns MD simulation with harmonic constraints on the protein heavy atoms with a force constant of $k = 1000$ kJ mol^{-1} nm^{-2} to equilibrate water and ions. Force-clamp MD simulations were performed with different constant pulling forces, namely 200, 500, 1000, 1500, and 2000 pN, for 10 ns each. The force was applied to the terminal C-α atoms of $I27_{SS}^{trunc}$ in opposite directions. The end-to-end length of $I27_{SS}^{trunc}$ and the distance between DTT and $I27_{SS}^{trunc}$ converged during these simulations. The final structures served as the starting structure for Quantum Mechanical/Molecular Mechanical (QM/MM) simulations under the corresponding pulling force.

QM/MM simulations were carried out using the GROMACS-3.3.1/GAUSSIAN03[31] interface.[32] A total of 15 atoms were treated quantum mechanically, namely the side chains of two cysteines between which a disulfide bond forms, the thiolate anion of DTT and its vicinal atoms, and three link atoms[20] introduced into the three carbon−carbon bonds which divide the QM and MM regions (see Figure 1A). The functional B3LYP and the 6-31G* basis set

(14) Ribas-Arino, J.; Shiga, M.; Marx, D. *Angew. Chem., Int. Ed.* **2009**, *48*, 4190–4193.
(15) Mamathambika, B. S.; Bardwell, J. C. *Annu. Rev. Cell Dev. Biol.* **2008**, *24*, 211–235.
(16) Hogg, P. J. *Trends Biochem. Sci.* **2003**, *28*, 210–214.
(17) Fernandes, P. A.; Ramos, M. J. *Chemistry* **2004**, *10*, 257–266.
(18) Bach, R.; Dmitrenko, O.; Thorpe, C. *J. Org. Chem.* **2008**, *73*, 12–21.
(19) Bolhuis, P. G.; Chandler, D.; Dellago, C.; Geissler, P. L. *Annu. Rev. Phys. Chem.* **2002**, *53*, 291–318.
(20) Field, M. J.; Bash, P. A.; Karplus, M. *J. Comput. Chem.* **1990**, *11*, 700–733.
(21) Saen-Oon, S.; Quaytman-Machleder, S.; Schramm, V. L.; Schwartz, S. D. *Proc. Natl. Acad. Sci. U.S.A.* **2008**, *105*, 16543–16548.
(22) Hofbauer, F.; Frank, I. *Chemistry* **2010**, *16*, 5097–5101.
(23) Van Der Spoel, D.; Lindahl, E.; Hess, B.; Groenhof, G.; Mark, A. E.; Berendsen, H. J. *J. Comput. Chem.* **2005**, *26*, 1701–1718.
(24) Jorgensen, W. L.; Maxwell, D. S.; Tirado-Rives, J. *J. Am. Chem. Soc.* **1996**, *118*, 11225–11236.
(25) Nose, S. *Mol. Phys.* **1984**, *52*, 255–268.
(26) Hoover, W. G. *Phys. Rev. A* **1985**, *31*, 1695–1697.
(27) Parrinello, M.; Rahman, A. *J. Appl. Phys.* **1981**, *52*, 7182–7190.
(28) Nose, S.; Klein, M. L. *Mol. Phys.* **1983**, *50*, 1055–1076.
(29) Darden, T.; York, D.; Pedersen, L. *J. Chem. Phys.* **1993**, *98*, 10089–10092.
(30) Hess, B.; Bekker, H.; Berendsen, H. J. C.; Fraaije, J. G. E. M. *J. Comput. Chem.* **1997**, *18*, 1463–1472.
(31) Frisch, M. J. *Gaussian 03*, revision C.02; Gaussian, Inc.: Wallingford, CT, 2004.
(32) Groenhof, G.; Bouxin-Cademartory, M.; Hess, B.; De Visser, S. P.; Berendsen, H. J.; Olivucci, M.; Mark, A. E.; Robb, M. A. *J. Am. Chem. Soc.* **2004**, *126*, 4228–4233.

were applied. A time step of 1 fs was used, and bonds containing a hydrogen atom were constrained using LINCS.[30] Other parameters were identical to those listed above. A range of different constant forces were applied to the termini as described for the MM system. The accumulated simulation time for all QM/MM simulations was 20 ns.

2.2. Transition Path Sampling.

2.2.1. Order Parameter and Initial Path. Transition path sampling (TPS) was developed to overcome high free-energy barriers in complex environments.[19] Unlike umbrella sampling, it does not require a reaction coordinate R_C to be defined beforehand and allows us to directly determine rate constants instead of indirectly estimating them from the activation free energy by assuming a pre-exponential factor. This allowed direct comparison to experiments. Only one order parameter λ is needed to define the RS and product state (PS) regions. Here, λ is defined as $d1 - d2$, where $d1$ and $d2$ are the lengths of the original and the newly formed disulfide bond, respectively (Figure 1A). We specified the phase space with $\lambda < -0.12$ nm and $\lambda > 0.12$ nm as RS and PS, respectively, for low forces. We moved the definitions to more negative λ values for high forces ($\geq$1000 pN) to prevent the transition state (TS) from moving into the RS region.

To generate a first reactive trajectory for subsequent TPS, the DTT molecule was forced to stay close to the disulfide bond by imposing a distance restraint on the distance $d2$ in Figure 1A, with an equilibrium distance of 0.2 nm and a high force constant of 10 000 kJ mol^{-1} nm^{-2}. Thiol/disulfide exchange occurred within 5 ps of MD simulations even under a force as low as 200 pN. This reactive trajectory served as the initial path for TPS. The subsequent sampling (see below) allowed us to relax the path ensemble from this first possibly improbable pathway to an energetically more favorable ensemble of disulfide reduction paths.

2.2.2. Sampling. In our implementation of TPS in Gromacs, shooting moves, shifting moves, and diffusion moves[33] were employed with probabilities 33%, 33%, and 33%, respectively, to create new reactive trajectories. A diffusion move shifted the path by one time slice in an arbitrary direction and was applied to improve the statistics of computed observables, e.g. $C(t)$, the correlation of state populations in time (see Supporting Information). The momentum displacement and the time displacement were adjusted to give an acceptance of about 40% for shooting and shifting moves, respectively, ensuring an optimal efficiency of the sampling.[19] The reactive trajectories are already decorrelated after four trajectories were sampled. At each of the five different forces, at least 500 reactive trajectories, each up to 600 fs in length, were generated. Together with additional TPS in smaller windows along λ, reaction rates were calculated as described in detail in the Supporting Information.

2.2.3. Estimation of Committor Probability. A transition state is a configuration that has an equal probability of relaxing to RS or PS. By defining P_B as the probability of a configuration to convert into PS, also called the commitment probability or committor,[19] one can calculate the value of P_B of a configuration by initiating a finite number N of fleeting trajectories, here chosen to be 20, from that configuration and count the number x of trajectories which reached PS. Then, $P_B = x/N$. According to the central limit theorem, the standard deviation of P_B is $\delta = \{P_B(1 - P_B)/N\}^{1/2}$. Thus, δ is about 0.1, with $P_B = 0.5$ and $N = 20$.

3. Results and Discussion

3.1. Force-Dependent Reaction Rates. The rate of disulfide bond reduction by DTT has been found to exponentially increase with force in the range of 100 to 400 pN.[3] We computed an ensemble of transition paths for this redox reaction at forces covering and extending this range, namely from 200 pN to 2 nN, by QM/MM simulations combined with transition path sampling. The reaction center is shown in Figure 1A. The progress of the reaction can be monitored in terms of the order parameters $d1$, the length of the originally formed disulfide bond in I27, and $d2$, the length of the newly forming disulfide bond between DTT and I27. From TPS, we obtained for each force at least 500 reactive trajectories for the redox reaction, representative examples of which are shown for 200 pN in Figure 1B. The disulfide exchange reaction clearly features an associated mechanism, with DTT approaching the stretched disulfide bond (measured by $d1$) largely prior to the extension and final rupture of the pulled disulfide bond ($d2$), as previously predicted for this reaction.[18]

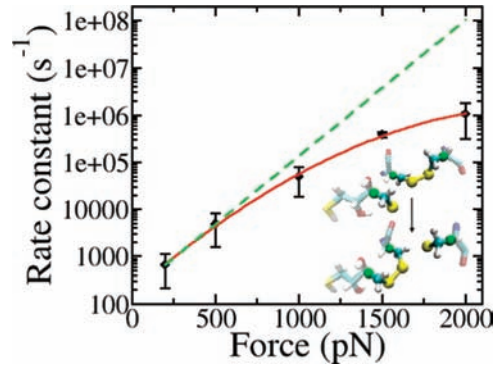

Figure 2. Rate constants estimated by TPS. Black diamonds: data from TPS, with the standard deviation shown as error bars. Red line: fit using the Dudko model ($\upsilon = 1/2$); Green dashed line: fit to the two low force data points using the Bell's model.

TPS offers the unique advantage of directly calculating reaction rates, in contrast to other common QM/MM sampling schemes such as umbrella sampling, which typically require the assumption of a pre-exponential factor for rate estimations. We in the first step validated our simulated force-dependent path ensemble by calculating reaction rates for direct comparison with experiment. Details on the rate calculations are given in the Supporting Information. Computed force-dependent rates are shown in Figure 2. As a first validation of our approach, the redox rates steadily increase with force. More specifically, this increase is highly nonlinear, with a weakening effect of the force on the rate at higher forces. This tendency is expected and previously has been both observed[14,34] and theoretically predicted.[11]

We next calculated concentration-dependent reaction rates. With the singly depronated DTT molecule being constrained to a volume of 1 nm^3 and considering the pK_a of the thiol group, we obtained a rate constant of 14 M^{-1} s^{-1} at 200 pN (see Supporting Information). Remarkably, the calculated rate is of the same order of magnitude as the experimental value, 27.6 M^{-1} s^{-1}. We thus conclude that our QM/MM model is able to reproduce the experimental rates. To our knowledge, this is the first time that QM/MM simulations have been used to successfully predict reaction rates. We here corrected for the very high effective concentration of DTT in our simulations compared to the experiments, which virtually neglects the diffusion of DTT to the reaction center. We then used Bell's model, with $r(F) = r_0 \exp[\beta F \Delta x_r]$, where $\beta = k_B T$, r_0 is the rate constant without external force, and F is the force, to estimate the distance between reactant and transition state, Δx_r, from the rates. For

(33) Van Erp, T. S.; Moroni, D.; Bolhuis, P. G. *J. Chem. Phys.* **2003**, *118*, 7762–7774.

(34) Dudko, O. K.; Mathe, J.; Szabo, A.; Meller, A.; Hummer, G. *Biophys. J.* **2007**, *92*, 4188–4195.

Table 1. Mechanical Parameters of the Disulfide Bond Reaction Obtained from Experiments[3] and Our QM/MM-TPS Simulations[a]

Model	Δx_r (Å)	ΔE_a (kJ/mol)	v
Dudko's	0.31	28[b]	1/2
Dudko's	0.28	25[b]	2/3
Exp.	0.34	30−65	−

[a] Parameters were estimated from simulations using Dudko's model[11] and least square fitting. [b] The value of $\Delta G^{\ddagger}$.

the whole force range of 200−2000 pN, we obained $\Delta x_r = 0.17$ Å, which is a clear underestimation of the experimental value ($\Delta x_r = 0.34$ Å). However, if we only take rates into account which cover the experimental range, namely those at 200 and 500 pN, Δx_r was estimated to be 0.28 Å and thus was consistent with experiments (Figure 2, green dashed line). The clear discrepancy of our Δx_r estimated by Bell's model and the experimental one demonstrates the failure of Bell's model in the description of the behavior of rate constants under high forces. More appropriate for the large range of forces employed here is the model devised by Dudko et al.[11] This model takes the shift of the transition state position due to the application of force into account as well as the shape of the potential energy factor, which introduces an additional parameter v. Then the force-dependent rate constant is given by

$$r(F) = r_0(1 - vF\Delta x_r/\Delta G^{\ddagger})^{1/v-1} \exp\{\beta\Delta G^{\ddagger} \times [1 - (1 - vF\Delta x_r/\Delta G^{\ddagger})^{1/v}]\} \quad (1)$$

Here, $\Delta G^{\ddagger}$ donates the apparent free energy of activation. Independent from the choice of v, we obtained a Δx_r convincingly close to the experimental value and an activation barrier of 25−28 kJ/mol, which falls into the experimental range as well (Table 1).

Overall, we conclude that both the absolute reaction rates and the force-dependency of our simulated redox reaction system are in good quantitative agreement with the available experimental data. The excellent fit of the Dudko model to our data suggests that the transition state moves toward the reactant state with increasing force, the molecular details of which can now be analyzed on the basis of our transition path ensemble.

3.2. Evidence for a Force-Dependent Transition State Structure. A shift of the TS with force toward the reactant state has been theoretically predicted[11,35] and experimentally observed.[12,34] Recently, calculations of a cis−trans isomerization provided further evidence for force-sensitive transition states.[14] More specifically, the potential energy landscape showed maxima which moved toward the reactant state with force. Here, we aimed at assessing the force-dependent TS structures on the *free energy* landscape of disulfide bond cleavage, with all dynamic, quantum, and solvent effects included.

To identify the ensemble of TS structures, we estimated the committor probabilities of conformations along transition paths. The committor probability, P_B, is the probability of a certain point in configuration space to commit to the product region *B*. We estimated P_B for a total number of 1595 structures taken from the ensemble of reactive trajectories, with roughly an equal number of structures for each force. A representative reactive trajectory is shown in Figure 3A, along with the committor probabilities P_B calculated for a subset of conformations visited on this path. For extended periods of time at the beginning and at the end of the trajectories, each spanning roughly 300 fs, the conformations exclusively commit to the reactant and product regions, respectively, an indication of a single-barrier crossing. In the intermediate time interval, the committor probabilities increase strongly nonmonotonically with time, especially in the range of $P_B \in [0.4,0.6]$, with several crossings of $P_B = 0.5$. In fact, most of the paths in the computed transition path ensemble showed more than one crossing of the separatrix, which has been previously observed for another diffusive biochemical reaction system.[21] Overall, the computed trajectories of committor probabilities feature all the characteristics of a diffusive single-barrier crossing, including a diversity of both reactive trajectories (see Figure 1B) and the TS structures (see Supplementary Figure 2) as one would expect for the S_N2 disulfide bond exchange reaction considered here. This is in agreement with the single exponential kinetics observed experimentally for disulfide bond cleavage, and in contrast to the static disorder causing nonexponential kinetics of protein folding over multiple barriers under force.[36]

Given a standard deviation of ∼0.1 for P_B of TS (see Methods), we considered all structures with $P_B \in [0.4,0.6]$ to be part of the TS ensemble. For each of the five forces, the resulting ensemble of TS structures was projected onto $d1$ and $d2$ (Supplementary Figure 2). Several ensemble averaged order parameters of the TS regions are given in Supplementary Table 2. We compared the geometry of the TS as observed here using QM/MM and TPS at the lowest force of 200 pN to those reported previously using quantum mechanical optimization methods. The study on the reduction of di-*tert*-butyl disulfide by *tert*-butyl mercaptide revealed a TS with $d1 = 2.52$ Å and $d2 = 2.67$ Å (both determined in implicit solvent) and an attack angle of 163.2° (determined in vacuum),[18] all of which are comparable to those observed here under 200 pN, with $d1 = 2.71$ Å, $d2 = 2.54$ Å, and $\alpha = 164°$. The force-dependent TS regions obtained from averaging over the TS structures at each force are shown in Figure 3B, again projected onto $d1$ and $d2$. They show a noticeable trend toward the RS with increasing force, reflected by a decrease of $d1$ and an increase of $d2$. Thus, mechanical force reduces the degree of disulfide bond opening ($d1$) and the extent of DTT attack ($d2$) that the system needs to get through to the transition state; i.e., the transition state is reached earlier. To our knowledge, this is the first evidence of a force-induced movement of the TS toward the RS on a free energy landscape at atomic resolution.

An exception from the force-induced shift is the TS at 1500 pN, which overlaps with the one at 200 pN in the projection onto $d1$ and $d2$ (Figure 3B). By examining the details of the corresponding TS ensemble, we found a pronounced difference in the dihedral around the original disulfide bond ϕ (see Figure 1B) at 1500 pN (221°) from those at the other four forces (<180°). Apparently, we sampled pathways at 1500 pN which were different from those at other forces. To clarify this, we investigated the distribution of dihedrals at different forces in the RS by classical MD simulations. At low forces, ϕ populates a single minimum below 180°, while, at forces beyond ∼400 pN, a second minimum >180° is populated (Supplementary Figure 3). We in all cases except 1500 pN sampled trajectories starting from an RS with $\phi < 180°$, which we therefore assume to correspond the preferred pathway. We argue that forces as high as 1500 pN can cause an originally unfavored pathway to

(35) Bustamante, C.; Chemla, Y. R.; Forde, N. R.; Izhaky, D. *Annu. Rev. Biochem.* **2004**, *73*, 705–748.

(36) Kuo, T.; Garcia-Manyes, S.; Li, J.; Barel, I.; Lu, H.; Berne, B.; Urbakh, M.; Klafter, J.; Fernández, J. *Proc. Natl. Acad. Sci. U.S.A.* **2010**, *107*, 11336–11340.

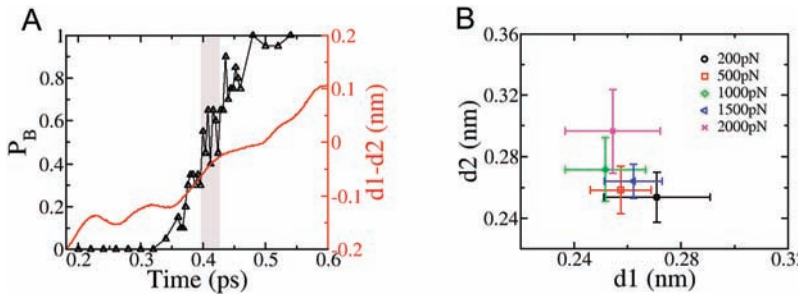

Figure 3. Identification of the TS region. (A) Committors P_B versus time for one representative disulfide bond cleavage path obtained at 2000 pN. The lifetime of TS, indicated by a gray shadow, is about 30 fs. (B) TS regions at varying forces, obtained from averaging over all structures with $P_B \in [0.4,0.6]$. Error bars are standard deviations. The mechanical force shifts the transition state region toward the reactant state, i.e. to larger $d2$ and smaller $d1$ values.

become feasible.[2,14] Sampling this second alternative pathway that differs in the dihedral distribution ϕ resulted in a different TS region. It nevertheless yielded a reasonable rate constant, conceivably because the two alternative pathways differing in ϕ of RS are roughly equally populated at 1500 pN. This discussion highlights the limitations of the TPS technique: the ensemble of transition paths is biased by the choice of initial configurations and starting trajectories in the case of multiple reaction channels, even though the size of the path ensemble was 2 orders of magnitude larger than the number of trajectories along which they decorrelate. Enhanced sampling methods combined with TPS like replica exchange might help to alleviate this issue. Overall, in spite of the convergence issue, both reaction rates and transition states are in agreement with previous studies, as detailed above, giving us confidence that our sampling covered the most essential parts of the transition path ensemble.

3.3. Relevant Order Parameters. The TS structures identified by a committor probability close to 0.5 were broadly distributed along both $d1$ and $d2$, even when considering only those observed at a single force (Supplementary Figure 2), resulting in the large standard errors in Figure 3B. Obviously, neither $d1$ nor $d2$ alone can represent the reaction coordinate (R_C) for the S_N2 reaction. We here employed a maximum likelihood approach recently developed by Peters et al. to identify the order parameters relevant for R_C.[37] Out of nine coordinates as candidates (see Supplementary Figure 4), we obtained $d1$, $d2$, ϕ, and the force F to contribute to R_C, in the form of a linear combination of them (see Supporting Information).

However, this approximate R_C has been only determined from structures of reactive trajetories, i.e. from a subconfiguration space, and might not be valid for the whole configuration space. Indeed, we tested the R_C by calculating committor distributions for those structures with $R_C = 0$ at $F = 200$ pN and found them to peak at 1 rather than 0.5 (Supplementary Figure 5). Hence, the R_C determined here is oversimplified and likely to neglect other crucial and maybe collective order parameters, such as the solvent. However, the four order parameters identified by this method must be highly relevant to the reaction coordinate, as their simple combination describes the process of this reaction very well in the subconfiguration space (see Supporting Information and Supplementary Figure 6). As expected, the intersulfur distances $d1$ and $d2$, which monitor the cleavage and formation of the original and new disulfide bonds, are relevant to the reaction coordinate. Less intuitively, ϕ is apparently also a crucial order parameter for the reaction.

(37) Peters, B.; Beckham, G. T.; Trout, B. L. *J. Chem. Phys.* **2007**, *127*, 034109.

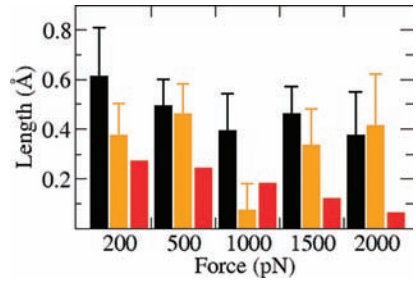

Figure 4. Comparison of geometrical parameters $\Delta d1$ and $\Delta d1z$ with the susceptibility of the redox reactivity to mechanical force as measured by Δx_r. Black, $\Delta d1$; yellow, $\Delta d1z$ (both averaged over the RS and TS ensemble; error bars are standard deviations); red, Δx_r (from the slope in Figure 2).

As already evident from the impact of force on the rate (Figure 2) and the TS structure (Figure 3B), force is another essential variable for the disulfide reduction.

3.4. Interpretation of Δx_r. The increase of the rate with force, as measured by Δx_r, is commonly interpreted as the distance from the reactant to the transition state along the pulling direction. For the disulfide-DTT exchange reaction, Δx_r has been directly associated with $\Delta d1$, the length change of the cleaving bond from RS to TS.[3] Now, having the structural ensemble of both the RS and TS at hand, we can systematically compare structural parameters like $\Delta d1$ with Δx_r.

As shown above, independent from the details of the fit, we found a Δx_r of ~0.3 Å. To reflect the steady decrease in the acceleration of the reaction by force, we also determined a force-dependent Δx_r, i.e. the susceptibility of the chemical reactivity to force, from the slope in Figure 2 (shown in red in Figure 4). We next measured $\Delta d1$ from the average bond length change we observed in the force-dependent ensembles of transition paths. As expected from the most simple picture where $\Delta x_r = \Delta d1$, we observe a slight tendency of $\Delta d1$ to shorten with force in a similar order of magnitude as Δx_r (Figure 4). However, this tendency is not significant, and the values of $\Delta d1$ are overall higher by roughly a factor of 2. In other words, the susceptibility of the reaction to forces is smaller than what is expected from the geometry of the RS and TS. To test if an angle $\theta > 0$ between $d1$ and the force vector leads to this deviation, we projected $d1$ onto the pulling direction z and compared the resulting $\Delta d1z$ to Δx_r. At 200 pN $\Delta d1z$ was 0.37 ± 0.13 Å, and thus very close to the Δx_r measured by experiments and observed in our calculations (compare Table 1). However, $\Delta d1z$ does not show the monotonic decrease with force. In fact, the decrease of $\Delta d1z$ with force is lost upon the projection, because force enhances the alignment of the disulfide bond with the pulling direction z.

Apparently, Δx_r cannot be straightforwardly related to changes in the geometry from the RS to TS.

4. Conclusions

For the interpretation of the pioneering experiments of the thiol/disulfide exchange reaction under force-clamp using single molecule force spectroscopy, a molecular picture including the force-sensitive quantum and dynamic effects is required. We investigated this reaction in atomic detail by dynamically sampling the reactive transitions using a QM/MM description of the reaction system in explicit solvent and TPS. We were able to validate our approach by directly estimating force-dependent reaction rates for this chemical reaction from our extensive nanosecond scale simulation data. Both the absolute rates and their force-dependency were close to the experimental values.

Proton exchange has been shown to play a role in the thiol/disulfide bond reaction.[22] However, the current implementation of the QM/MM interface does not allow us to consider any protonation or deprotonation as a step of the reaction. We instead consider a deprotonated DTT molecule as the reactant and corrected for this in the rate calculations. The agreement of the calculated force-dependency with the experimental data further implies that the proton exchange steps are largely force-independent. Investigating the interesting question of the susceptibility of proton exchange reactions to mechanical forces is required to test this.

We demonstrated that, even for the simple case of the reduction of a protein disulfide bond by DTT, a nonexponential dependency of the rates with force in the range of 200 to 2000 pN can be expected. We predict the general aspects of our findings, namely (i) a pronounced shift of the TS toward the RS along $d1$ and $d2$ and (ii) a complex multidimensional reaction coordinate, to be also valid for other reducing agents experimentally tested so far, such as thioredoxin. In fact, the only reaction probed up to 2 nN so far does not show any evidence of a transient TS shift but instead an abrupt switch between mechanisms.[6] While further theoretical investigations are required to understand this particular case of hydroxide nucleophilic attack, increasing the time resolution of AFM experiments might allow us to test our predictions for thiol/disulfide exchange with DTT at high forces. Similarly, experiments using a thiol-based reducing agent with lower nucleophilicity, e.g. by multiple fluorination, can be expected to reveal the shift in the TS structure predicted by our study. Our QM/MM-TPS approach can be easily transferred to other redox systems and (bio)chemical reactions to test this prediction.

A major conclusion from our findings is that care must be taken when relating the measured Δx_r to single geometric parameters of the reaction system like a bond length. We here found Δx_r not to correlate with any of the order parameters playing a role in the redox reaction but instead to reflect a measure in the sensitivity of the S_N2 reaction to force that depends on how force distributes through the various order parameters of the multidimensional reaction coordinate. As a consequence, neglecting other degrees of freedom and assuming the mechanical work to be solely performed along the direction of the cleaving bond would lead to an overestimation of the effect of force on the reactivity. We predict the propagation of force onto degrees of freedom orthogonal to the pulling direction to be a general characteristic for reaction centers in condensed systems.

Acknowledgment. The authors thank Wolfram Stacklies for sharing his GROMACS code for constant force pulling, Fei Xia and Shanmei Cheng for fruitful discussions, Gerrit Groenhof for help with the Gromacs-Gaussian interface, and together with Ilona Baldus for carefully reading the manuscript. W.L. is grateful for an MPG-CAS PhD scholarship.

Supporting Information Available: Complete refs 8 and 31, details of rate calculations including figures, and tables of TS and RS structures. This material is available free of charge via the Internet at http://pubs.acs.org.

JA104763Q